Tetrahedron 67 (2011) 8120–8130

Contents lists available at SciVerse ScienceDirect

Tetrahedron

journal homepage: www.elsevier.com/locate/tet

Metallomesogens derived from benzoxazoles–salicylaldimine conjugates

Chun-Jung Chen [a], I-Wen Wang [a], Hwo-Shuenn Sheu [b], Gene-Hsiang Lee [c], Chung K. Lai [a,*]

[a] Department of Chemistry and Center for Nano Science Technology, National Central University, Chung-Li 32001, Taiwan, ROC
[b] National Synchrotron Radiation Research Center, Hsinchu 30077, Taiwan, ROC
[c] Instrumentation Center, National Taiwan University, Taipei 10660, Taiwan, ROC

ARTICLE INFO

Article history:
Received 6 June 2011
Received in revised form 13 August 2011
Accepted 19 August 2011
Available online 25 August 2011

ABSTRACT

The synthesis, characterization, and mesomorphic properties of a new series of Schiff bases **2a–h** and metal complexes **1a–h–M** are prepared and their mesomorphic properties studied. Two single crystallographic structures of **2d** (n=12, m=1) and **1g–Pd** (n=m=12) were determined by X-ray analysis. Both compounds crystallize in a triclinic space group $P-1$. A dimeric structure formed by *intermolecular* H-bonds in **2d** was observed, giving nematic phase due to a better aspect ratio. The central geometry at Pd^{2+} ion is nearly perfect square plane. All Schiff bases **2a–h** formed N or/and SmC phases. The formation of mesophases of complexes **1a–h–M** was strongly dependent on metal ions incorporated. All Cu^{2+}, Ni^{2+} and Pd^{2+} complexes exhibited N or/and SmC phase, respectively. However, Zn^{2+} and Co^{2+} complexes were not mesogenic. The lack of mesomorphism was probably attributed to a preferred tetrahedral geometry at Zn^{2+} and Co^{2+} over a square-planar geometry at Cu^{2+} and Pd^{2+}.

1. Introduction

The coordination geometry of metal ions as core center incorporated in metallomesogenic materials[1] has been demonstrated to play a key element in controlling or inducing the formation of mesophases. Coordination complexes[1] constitute the largest category among the known metallomesogens, in which numerous metallomesogens with unique geometric structures and novel mesomorphic behavior were thus generated by incorporating appropriate metal ions. In general, the overall molecular shape[1f,g,i] of a particular compound was closely determined by the geometry of central metals and/or also surrounding organic moieties. The coordination numbers (CN) of metal ions are virtually diverse, which are often correlated with their oxidation states/electronic states. For example, M^{2+} ions have a CN=4, while M^{3+} ions have a CN=6. Metallomesogens with a CN=4 are mostly known, of which a geometry of either tetrahedral or square-planar geometry is all possible. Complexes with a square-planar geometry give preferably rise to liquid crystallinity, whereas complexes with a tetrahedral geometry are usually not mesogenic due to their unfavorable packing. However, a few tetrahedral complexes[1a] were in fact mesogenic, giving columnar or nematic structures in LC states. Metal ions, such as diamagnetic d^8-Ni^{2+} and d^8-Pd^{2+}/Pt^{2+} ions generate square planar complexes, while paramagnetic d^7-Co^{2+} and d^{10}-Zn^{2+} ions preferably give tetrahedral complexes. On the other hand, paramagnetic d^9-Cu^{2+} ions, depending on the organic moiety can be either tetrahedral, twisted square planar or perfectly square planar at central geometry.

Benzoxales or 2-(*o*-hydroxylphenyl)-2-benzoxales (HPBs), grouped as a member of heterocyclic derivatives have been applied to construct a variety of novel mesophases previously in this group[2] and others.[3] The formation of liquid crystallinity was found to be favored by π–π interactions and/or H-bonds induced in such structures. Higher polarization was induced by incorporation of heteroatoms, such as N, S, and O atoms, which often facilitate the formation of mesophases. *Intramolecular* or/and *intermolecular* H-bonds might be possibly induced by H···N, H···S or H···O atoms. An *intramolecular* or/and *intermolecular* force polarized by donor and acceptor interaction (D→A) between the electron-deficient five-membered ring and neighboring electron-rich phenyl or aromatic rings was often observed. In addition, nonplanar core structures can lead to lower symmetries, giving lower melting and/or clearing temperatures required for potential device applications. Most of known mesogenic benzoxales[2,3] exhibited nematic and/or smectic A/C phases, as expected for linear-shaped molecules. The formation of mesophases in such electron-deficient benzoxales was found to be greatly affected by polar substituents.[2] Like oxadiazoles, they have been studied due to their interesting spectroscopic and photophysical properties. The HPB molecules showed luminescent properties,[4] which were useful in organic light-emitting diodes (OLEDs). A few metal complexes[5] derived from HPBs, such as iridium(III),[5a] vanadyl(IV),[5b] zinc(II),[5c] and ruthenium(II)/osmium(II)[5d–f] were known and their structures characterized. However, only one metallomesogen[6] (i.e., Cu^{2+}, Pd^{2+}) derived from

* Corresponding author. Tel.: +886 3 4259207; fax: +886 3 4277972; e-mail address: cklai@cc.ncu.edu.tw (C.K. Lai).

0040-4020/$ – see front matter © 2011 Elsevier Ltd. All rights reserved.
doi:10.1016/j.tet.2011.08.048

benzoxales was reported by this group.[6a] Both complexes exhibited N or/and SmC phases over a wide range of mesophases.

Transition metal complexes derived from salicylaldimines[7] were among one of the most known complexes that exhibited mesogenic properties in metallomesogens. Almost all 3d transition metal complexes derived from salicylaldimines[1h] exhibited mesomorphic properties. A tetrahedral or square-planar geometry in [O_2,N_2]-chelating fashions of salicylaldimines is often found for complexes with a CN=4. Pd^{2+}/Pt^{2+} ions prefer square-planar geometries, while Co^{2+} and Zn^{2+} ions form tetrahedral geometries. Cu^{2+} ions can coordinate by either tetrahedral or square-planar geometries. Most of reported metallomesogens with a CN=4 were more likely rod-shaped molecules, exhibiting nematic and/or layered smectic phases, while few complexes[7a,7t] with more disc-shaped molecules formed columnar phases. Known metallomesogens with octahedral geometries[1b,8] obtained by incorporating Mn^{3+}/Cr^{3+}/Co^{3+}/Fe^{3+} ions or others exhibiting columnar phases were relatively limited. In this work, as part of our continuing research on exploring new metallomesogens, a new series of benzoxazole–salicylaldimine conjugates **2a**–**h** and their transition metal complexes **1a**–**h**–**M** were prepared. In order to comprehend the effect of the geometry of metal ions incorporated, cobalt, nickel, palladium, zinc, and copper complexes were prepared. Results showed that Cu^{2+}, Ni^{2+}, and Pd^{2+} complexes exhibited N or/and SmC phase. However, Zn^{2+} and Co^{2+} complexes were all crystalline. The lack of mesomorphism was attributed to a preferred tetrahedral geometry at Zn^{2+} and Co^{2+}.

2. Results and discussion

2.1. Synthesis and characterization

The synthetic pathways[9] to benzoxazoles **2a**–**h** and their metal complexes **1a**–**h**–**M** (M=Co, Ni, Cu, Zn, Pd) are summarized in Scheme 1. Most benzoxazoles were prepared by the condensation of 2-aminophenols with benzaldehydes or benzoic acid and subsequent intramolecular cyclization. In this work, 2-(4-alkoxyphenyl)benzoxazol-5-ylamines **3** were similarly prepared by our previous procedures.[6a] The Schiff bases **2a**–**h** were obtained by reactions of amines **3** and 4-alkoxy-2-hydroxy benzaldehydes in refluxing absolute ethanol for 12 h. The yields were slightly increased with carbon lengths. ^{1}H and ^{13}C NMR spectroscopy were used to characterize all intermediates **2**–**4**. A singlet appeared at δ 8.53–8.55 ppm, characteristic of imine (−N=CH) was observed for the formation of compounds **2a**–**h**. The solvent-dependent ground-state conformational equilibrium and excited dynamic of 2-(2′-hydroxyphenyl)benzoxazole have been characterized in several solvents.[10] The only observable ground-state tautomers is the enol form, which exists in equilibrium between the *syn*- and *anti*-rotational isomers.

The metal complexes were prepared by the reaction of benzoxazole–imines **2a**–**h** and $M(OAc)_2$ (M=Co, Ni, Cu, Zn, Pd) in refluxing abs ethanol/THF for 2 h. Metal complexes, isolated as gray-green (Cu), yellow (Ni), light orange (Pd), pale-yellow (Zn), and brown (Co) solids were purified by a few times recrystallizations from THF/CH_3OH at room temperature. The yields were modestly ranged from 58 to 81%. Cobalt complexes were slightly sensitive to air, especially when dissolved in the solution. The elemental analysis was used to confirm the purity of Schiff bases **2a**–**h** and metal complexes **1a**–**h**–**M**.

2.2. Single crystal structures of 2d (*n*=12, *m*=1) and 1g–Pd (*n*=*m*=12)

In order to understand the correlation between the molecular structures and mesomorphic behavior, two single crystals of the mesogenic **2d** (*n*=12, *m*=1) and mesogenic **1g**–**Pd** (*n*=*m*=12) suitable for crystallographic analysis were obtained by slow diffusion from CH_2Cl_2/MeOH at room temperature and their structures resolved. Fig. 1 shows the two molecular structures with the atomic numbering schemes.

Table 1 lists their crystallographic and structural refinement data for the two molecules. Compound **2d** crystallizes in a triclinic space group *P*−1 with a *Z*=2. The overall molecular shape of **2d** was considered as linear-shaped with an overall molecular length of ∼33.438 (32) Å. As expected, an *intramolecular* H-bond between phenolic H2A⋯N2 atoms was observed, and the distance was measured by ca. 1.745 (7) Å. Also a few *intermolecular* H-bonds were observed in the crystal lattice. A dimeric structure with a length of ca. 53.28 Å in a head-to-head fashion was thus formed by H-bonds, and these H-bonds were relatively weak (Fig. 2). The H-bond lengths were ranged from *d*=2.541–2.669 Å. These weak H-bonds were consistent with nematic phase observed in **2d**. The formation of the dimeric structure was probably two-fold; a larger core induced and an elongated molecule were generated, leading to a better aspect ratio, as often required for mesogens. The induced conformation was believed to facilitate molecular packing both in the solid or/and the liquid crystal state. The benzoxazole, phenolic, and lateral phenyl rings were in fact not coplanar, with a small dihedral angle; 2.833 (164)–4.416 (157)°. The *intramolecular* H-bonding kept all three rings roughly coplanar, and the planar structure was responsible for a better packing. In the unit cell, all molecules were arranged by antiparallel and head-to-tail arrangements (Fig. 3). No π–π interaction, consistent with only nematic phase was observed in **2d**. Some selected bond lengths and bond angles are listed in Table 2. A layered structure was observed and the molecular arrangement in unit cell was shown in Fig. 3.

The complex **1g**–**Pd** (*n*=*m*=12) also crystallizes in triclinic space group *P*−1 with a *Z*=1. The geometry at palladium was coordinated as perfect square planar. The two angles of N1(#)–Pd–O1 and N1(#)1–Pd–O1(#) atoms were of 88.60 (9)° and 91.42 (9)°, which were close to an angle of 90° expected for a square-planar geometry. The overall molecular shape was considered as chair-shaped with a length of ca. 47.29 Å [i.e., C44–C44(#)]. The two central planes defined by N1–O1–Pd–O1–N1 atoms were coplanar. The benzoxazole ring and central Pd plane (by N1–O1–Pd–O1–N1) were not coplanar, with a dihedral angle of 70.692°. In the lattice, two molecules were attracted by a weak π–π interaction. A distance of ca. ∼2.863 Å as point-to-face alignment between the H17A of phenyl ring and central Pd plane was obtained. Two other weaker π–π interactions were also observed between the neighboring up-and-down molecules, and the distances were measured as 3.048 and 3.732 Å (Fig. 4). All alkoxy chains were interdigitated and the Van der Waal interaction between the alkoxy chains was observed. A layered structure observed in **1g**–**Pd** and the molecular arrangement in unit cell were shown in Fig. 5.

2.3. Mesomorphic properties

The liquid crystalline behavior of compounds **2a**–**h** and **1a**–**h**–**M** was characterized and studied by differential scanning calorimetry and polarized optical microscope. The phase transitions and thermodynamic data are summarized in Tables 3 and 4. All derivatives **2a**–**h** exhibited enantiotropic nematic or/and smectic C phases. Four derivatives **2a**–**d** appended with two shorter alkoxy chains formed nematic phases, while other three derivatives **2e**–**g** with two longer alkoxy chains formed nematic phase at higher temperature and smectic C phase at lower temperature. The derivative **2h** (*n*=12, *m*=16) showed SmC phase. This type of mesophase-dependence on the lateral carbon length is often observed in rod-like mesogens. Interestingly, the derivative **2a** with two $-OCH_3$ chains were truly mesogenic, which has been

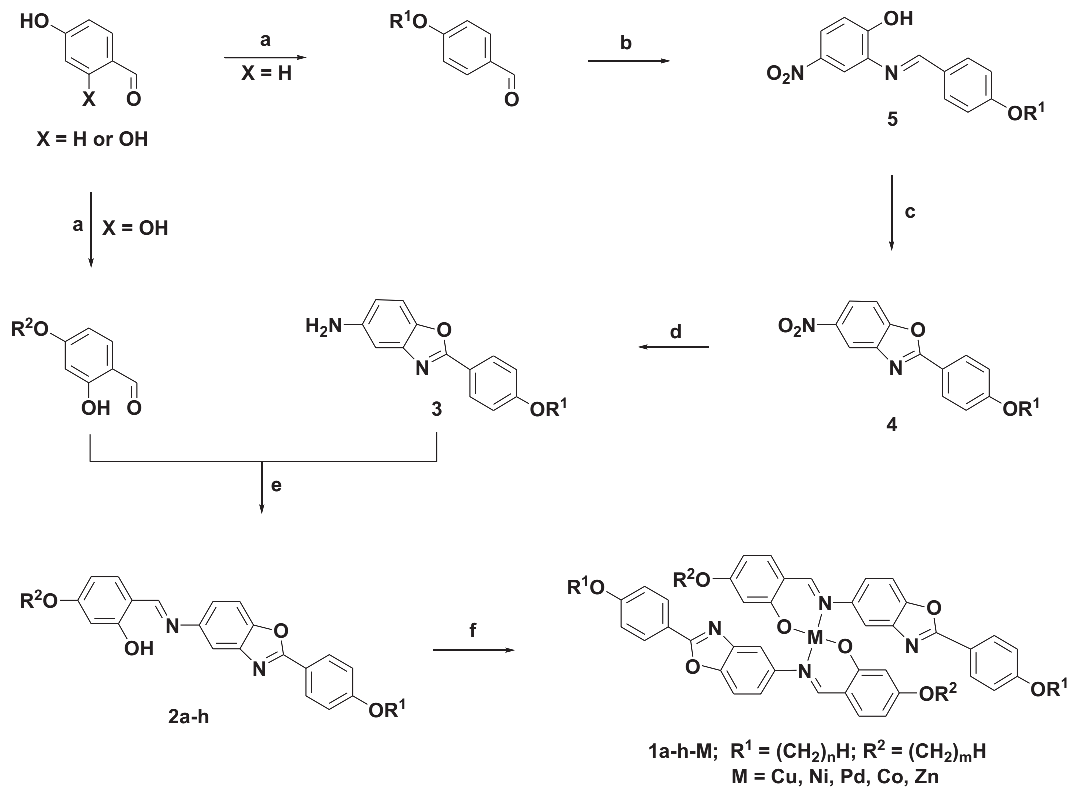

Scheme 1. Reaction and Reagents. (a) RBr (1.0 equiv), K_2CO_3 (1.5 equiv), KI (cat.), refluxing in dry CH_3COCH_3, 48 h; (b) 2-amino-4-nitrophenol (1.0 equiv), CH_3COOH (drops), refluxing in abs C_2H_5OH, 12 h; (c) $Pb(OAc)_4$ (1.3 equiv), refluxing in $CHCl_3$, 4 h; (d) N_2H_4 (1.1 equiv), Pd/C (0.1 equiv), refluxing in C_2H_5OH, 6 h; (e) CH_3COOH (drops), refluxing in dry C_2H_5OH, 12 h; (f) $M(OAc)_2$ M=Cu, Ni, Pd, Co (0.5 equiv), refluxing in abs C_2H_5OH/THF, 2 h.

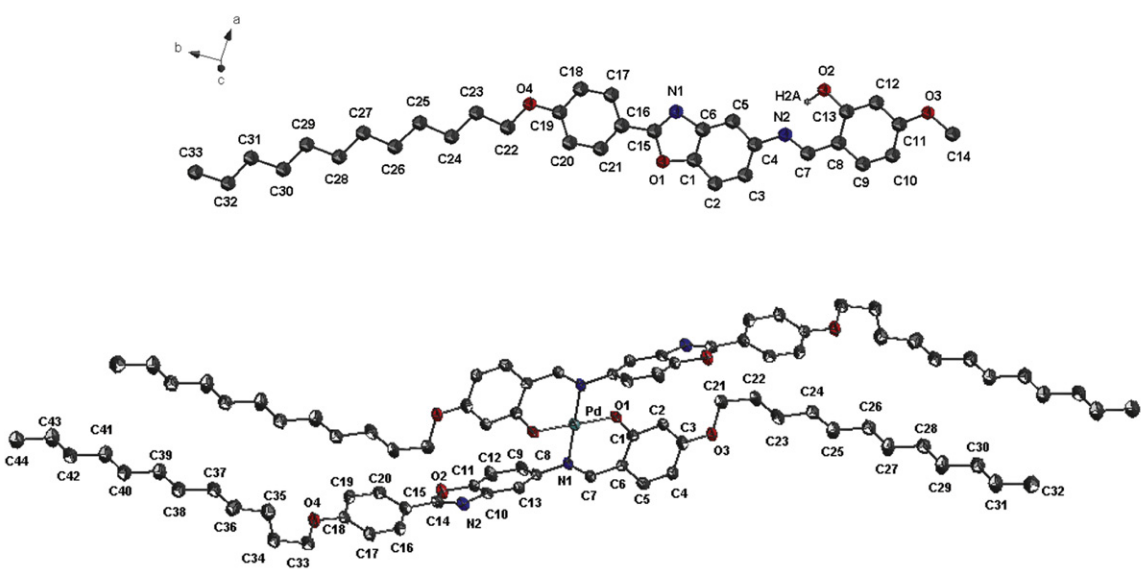

Fig. 1. Two ORTEP plots for compound **2d** (n=12, m=1) and **1g–Pd** (n=12, m=12) with the numbering scheme, and the thermal ellipsoids of the non-hydrogen atoms are drawn at the 50% probability level.

observed in other similar benzoxazoles.[6a] A higher clearing temperature of **2a** at T_{cl}=293.7 °C was observed due to its more rigid core and/or less flexible chains. **2a** showed slight decomposition at temperature higher than its isotropic point. Methoxy group is usually not considered as a flexible chain. The formation of nematic phases might be attributed to the more hindered conformation caused by two lateral phenyl rings. Its lesser coplanar core resulted from the tetrahedral methyl and also a free rotation between carbon–carbon single bond between the central and two lateral phenyl rings might induce the formation of ne2matic phase. The clearing temperatures decreased with increasing carbon lengths, T_{cl}=224.6 (**2c**)>200.6 (**2d**)>197.9 (**2e**)>185.2 (**2f**)>179.0 (**2g**)> 164.9 °C (**2h**). Single crystallographic analysis of **2d** showed that a dimeric structure was induced by H-bonds in a head-to-head fashion, indicating that the lower alkoxy chains (i.e., m value) merged into the two lateral alkoxy chains (i.e., n value) will not alter or affect much the overall molecular length. The temperature range of mesophase in **2** increased from a ΔT_{LC}=56.2 (**2h**)–110.0 °C (**2c**) on the heating process. Both derivatives **2b** (n=1, m=12) and **2d** (n=12, m=1) showed similar mesomorphic behavior due to their

Table 1
Crystallographic and experimental data for compounds **2d** and **1g–Pd**

Compds.	**2d** (n=12, m=1)	**1g–Pd** (n=12, m=12)
Empirical formula	$C_{33}H_{40}N_2O_4$	$C_{88}H_{122}N_4O_8Pd$
Formula weight	528.67	1470.30
T/K	150 (2)	150 (2)
Crystal system	Triclinic	Triclinic
Space group	$P-1$	$P-1$
a/Å	8.6607 (11)	8.3188 (3)
b/Å	12.7815 (15)	10.1646 (3)
c/Å	14.3162 (16)	23.2657 (7)
α/°	66.610 (5)	93.3681 (18)
β/°	75.484 (7)	93.407 (2)
γ/°	78.191 (7)	93.1423 (15)
U/Å^3	1935.0 (2)	1957.06 (11)
Z	2	1
F(000)	568	788
D_c/Mg m^{-3}	1.256	1.248
Crystal size/mm^3	0.70×0.06×0.03	0.25×0.17×0.02
Range for data collection/°	1.58–25.00	1.76–25.00
Reflection collected	14,454	25,339
Data, restraints, parameters	4892/0/355	6860/0/457
Independent reflection	4892 [R(int)=0.1217]	6860 [R(int)=0.0763]
Final $R1$, $wR2$	0.1047, 0.2749	0.0525, 0.1082

Pd^{2+} complexes exhibited N or/and SmC phase, respectively. Both Co^{2+} and Zn^{2+} complexes were crystalline. All complexes (except complex **1g–Ni**) have higher clearing temperatures than those of free Schiff bases **2a–h** due to their larger core sizes or molecules. The clearing temperatures of all complexes formed, for example, with same derivative **2g** decreased in the order of T_{cl}=224.4 (Pd)>200.2 (Zn)>198.8 (Co)>197.2 (Cu)>174.2 °C (Ni). The transition temperatures for some derivatives **1–M** are not observed on DSC analysis, therefore they were obtained by optical microscope. Surprisingly, complex **1a–Cu** (n=m=1) was also mesogenic, exhibiting a nematic phase at T_{mp}=284.6 °C and T_{cl}=304.2 °C. This complex showed slightly decomposition at temperature higher than T_{cl}>304.2 °C. The temperature range of N phase, ΔT_N=19.6 °C was relatively short on heating process. The clearing temperatures of complexes **1a–h–Cu** in this series decreased with increasing carbon length, i.e., T_{cl}=304.2 (**1a–Cu**)>255.6 (**1c–Cu**)>223.1 (**1e–Cu**)>192.6 °C (**1h–Cu**). Both two complexes **1g–Cu** and **1h–Cu** formed only smectic C phases. The nematic and smectic C phases were identified by microscope. A typical texture described as focal-conic or Schlieren domains (Fig. 6) were observed under POM when cooling from isotropic liquid. Nickel and palladium formed similar mesomorphic behavior as copper complexes.

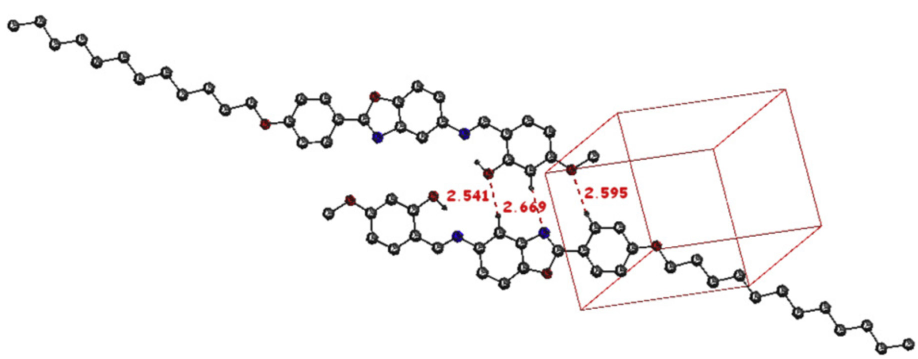

Fig. 2. A dimeric structure formed by *intermolecular* H-bonds in **2d** (n=12, m=1).

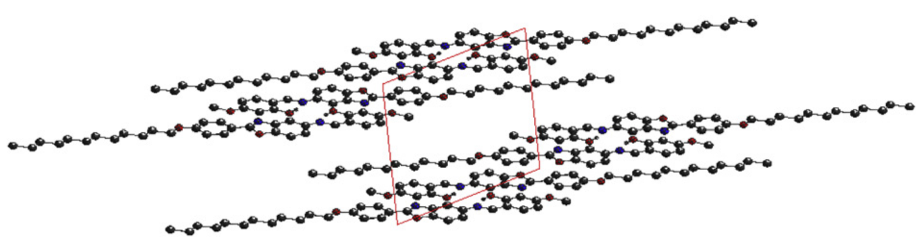
Fig. 3. The molecular arrangements in **2d** when viewed from a-axes.

approximately equal overall molecular lengths. The temperature range of N phase decreased with increasing carbon lengths, for example, ΔT_N=122.6 (**2c**)>95.1 (**2d**)>32.0 (**2e**)>211.3 (**2f**)>2.6 °C (**2g**), whereas, the temperature range of smectic C phase remained from ΔT_{SmC}=94.6 (**2f**)–69.7 °C (**2h**). The phases were identified as N and smectic C phase by POM. A typical texture as Schlieren domains for N phase, or fan-shaped or Schlieren for SmC phase were observed under optical polarized microscope when cooling from isotropic states (Fig. 6). Optical textures of SmC phase were not homeotropic, which were often observed in SmA and N phases. A lower enthalpy, i.e., ΔH=0.26–2.26 kJ/mol for the transition of N→I phase was obtained. The formation of N phases was also quite consistent with molecular packing, as seen from single crystal analysis.

On the other hand, complexes **1a–h–M** showed a strong dependence of metal ions incorporated on the formation of mesophases. Cu^{2+}complexes formed N or/and SmC phases, and Ni^{2+} and Complexes **1–Pd** have higher clearing temperatures then those of **1–Ni**, which might be attributed to the stronger coordinative interaction between the neighboring molecules in Pd over than in Ni complexes. All Zn^{2+} and Co^{2+} complexes were not mesogenic. A transition from crystal-to-isotropic at T_m=200.2 °C and T_m=198.8 °C, for **1g–Zn** and **1g–Co**, respectively, was observed. Both Zn^{2+} and Co^{2+} ions often prefer tetrahedral coordinations. The lack of mesomorphism was probably attributed to the tetrahedral geometry, in which molecules were unfavorable to pack in a more regular arrangement required for mesogens.

2.4. Variable-temperature powder XRD diffraction data

The powder X-ray diffraction experiments for two compounds **2g–h** and three complexes **1g–Cu** (n=m=12), **1h–Cu** (n=12, m=16), and **1g–Pd** (n=12, m=12) were performed to confirm the structures of the smectic C phases. The X-ray diffraction data were

Table 2
Selected bond distances [Å] and angles [°] for **2d** and **1g–Pd**

2d (n=12, m=1)			
Bond distances			
O(2)–C(13)	1.369 (6)	C(8)–C(9)	1.414 (7)
N(2)–C(7)	1.287 (6)	C(8)–C(13)	1.423 (7)
N(2)–C(4)	1.405 (6)		
Bond angles			
C(7)–N(2)–C(4)	122.9 (4)	C(9)–C(8)–C(7)	120.5 (4)
N(2)–C(4)–C(3)	125.1 (4)	C(13)–C(8)–C(7)	122.9 (4)
N(2)–C(7)–C(8)	122.1 (5)	O(2)–C(13)–C(8)	119.6 (4)
C(9)–C(8)–C(13)	116.6 (5)		
1g–Pd (n=12, m=12)			
Bond distances			
Pd–O(1)	1.954 (2)	C(1)–C(2)	1.410 (4)
Pd–N(1)	2.033 (3)	C(1)–C(6)	1.411 (4)
O(1)–C(1)	1.323 (4)	C(6)–C(7)	1.422 (4)
N(1)–C(7)	1.301 (4)	C(8)–C(9)	1.391 (4)
N(1)–C(8)	1.445 (4)		
Bond angles			
O(1)–Pd–O(1)#1	180.00 (10)	N(1)–C(7)–C(6)	127.6 (3)
O(1)–Pd–N(1)#1	88.60 (9)	C(9)–C(8)–N(1)	120.7 (3)
O(1)#1–Pd–N(1)#1	91.40 (9)	C(1)–O(1)–Pd	128.5 (2)
C(7)–N(1)–C(8)	117.8 (3)	C(7)–N(1)–Pd	123.4 (2)
C(8)–N(1)–Pd	117.86 (19)	O(1)–C(1)–C(2)	115.9 (3)
O(1)–C(1)–C(6)	123.6 (3)	C(2)–C(1)–C(6)	120.5 (3)
C(3)–C(2)–C(1)	119.8 (3)	C(1)–C(6)–C(7)	123.8 (3)

assigned to the molten alkoxy chains. The d-spacings of compounds **2g** and **2h** were quite close due to their similar structures in overall length. Powder XRD diffraction data of complexes **1g–Cu** (n=m=12), **1h–Cu** (n=12, m=16) and **1g–Pd** (n=12, m=12) showed similar diffraction patterns as SmC phases compounds **2g–h**. Both complexes have two diffraction peaks at 34.3 Å and 17.2 Å, and 36.9 Å and 18.5 Å assigned as index 001 and 002 for **1g–Cu** (n=m=12), **1h–Cu** (n=12, m=16), respectively. Complex **1g–Pd** (n=12, m=12) showed a similar d-spacing of 34.8 Å as that (~34.3 Å) of **1g–Cu** (n=12, m=12).

3. Conclusions

A new metallomesogens based on Ni^{II}, Co^{II}, Cu^{II}, Pd^{II}, and Zn^{II} centers coordinated to benzoxazoles–salicylaldimine conjugates were prepared and their mesomorphic properties studied. An induced dimeric structure by H-bonds formed in single crystal **2d** (n=12, m=1) facilitates the formation of mesophases. Metal complexes derived from bidentate salicylaldimines adopted a preferred bonding fashion of [O_2,N_2]-donor atoms. Single crystal X-ray structural analysis of **1g–Pd** (n=m=1) confirmed a trans-square planar arrangement for palladium complex. A strong dependence of geometries of metal ions incorporated on the formation of mesophase was demonstrated. Metal ions, such as Cu^{2+}, Ni^{2+}, and Pd^{2+} coordinated by a square-planar geometry formed N or/and SmC phases. In contrast, Zn^{2+} and Co^{2+} complexes with a tetrahedral geometry were not mesogenic.

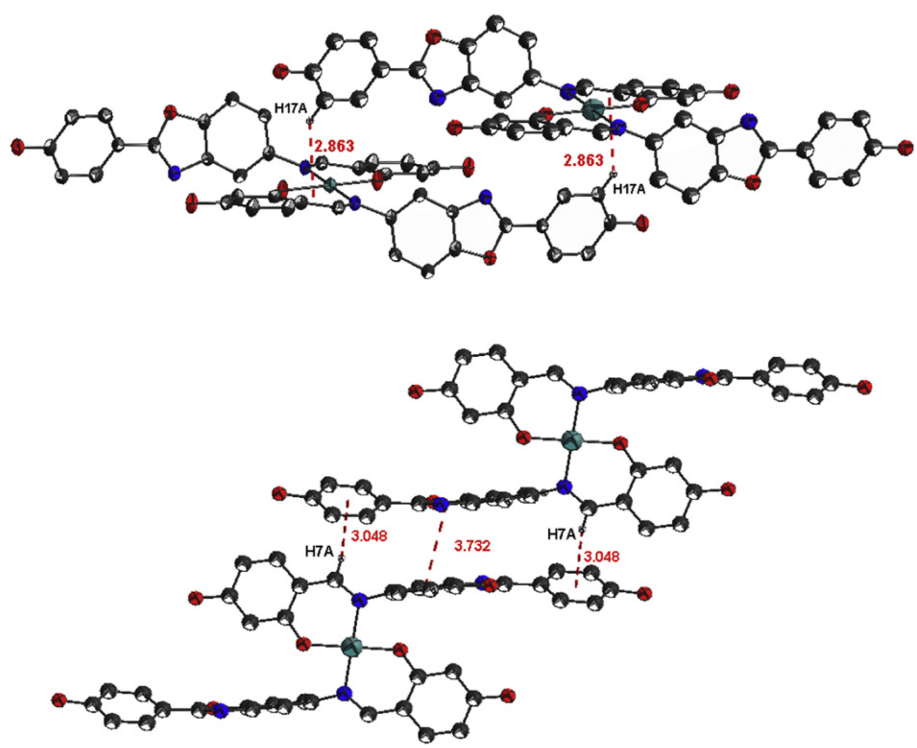

Fig. 4. The π–π interactions observed in **1g–Pd** (m=n=12).

summarized in Table 5. As indicated, they all displayed a similar diffraction pattern with one strong peak and/or one very weak at lower angle region, and also a very weak and broad diffraction peak at wider angle. The first two diffraction peaks appeared at lower angle were assigned as 001 and 002. This diffraction pattern was typically characteristic of a layer structure observed for SmC phases. For example, compound **2h** showed a strong peak at 39.8 Å and a weak peak at 19.9 Å, shown in Fig. 7. A d-spacing of 38.2 Å at 150 °C obtained for **2g** was much smaller than 47.1 Å obtained from calculated molecular length, which indicated the molecules were tilted and also the alkoxy chains were highly interdigitated. A very broad and weak peak at ~4.60 Å was observed, and this peak was

4. Experimental section

4.1. General

All chemicals and solvents were reagent grades from Lancaster or Aldrich. Solvents were dried by standard techniques. ^{1}H and ^{13}C NMR spectra were measured on a Bruker AM-300. FT-IR spectra were performed on Nicolet Magna-IR 550 spectrometer. DSC

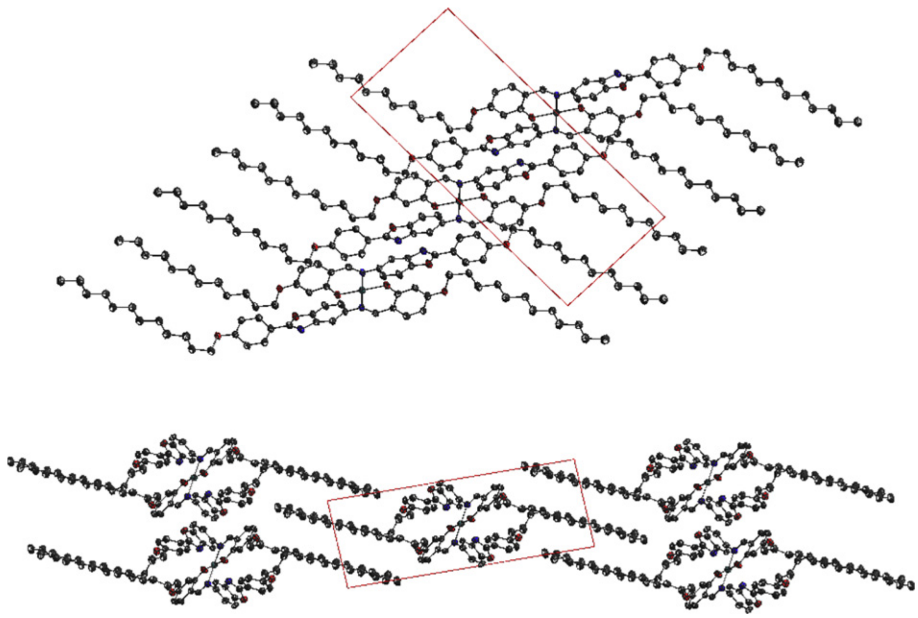

Fig. 5. Molecular arrangements in **1g–Pd** when viewed from *a*- and *b*-axes.

Table 3
Phase transitions and enthalpies[a] of compounds **2a–h**

	n	m		Heating / Cooling		Heating / Cooling		Heating / Cooling	
2a	n = 1	m = 1			Cr	217.3 (51.4) / 164.0[b]	N	293.7 (0.44) / 287.0[b]	I_d
2b	1	12			Cr	123.0 (39.0) / 109.5 (39.0)	N	202.8 (0.30) / 200.0 (0.29)	I
2c	8	1			Cr	114.6 (23.8) / 100.5 (23.6)	N	224.6 (2.26) / 223.1 (0.26)	I
2d	12	1			Cr	115.6 (39.8) / 103.7 (39.5)	N	200.6 (0.45) / 198.8 (0.43)	I
2e	12	4	Cr	103.1 (23.3) / 84.1 (23.0)	SmC	166.9 (0.24) / 163.4 (0.23)	N	197.9 (0.83) / 195.4 (0.72)	I
2f	12	8	Cr	100.0 (30.2) / 75.2 (30.0)	SmC	174.1 (0.93) / 169.8 (0.85)	N	185.2 (1.00) / 181.1 (0.98)	I
2g	12	12	Cr	105.4 (47.8) / 83.4 (46.8)	SmC	176.4 (2.25) / 175.3 (1.89)	N	179.0 (1.60) / 177.9 (1.44)	I
2h	12	16			Cr	108.7 (69.8) / 93.6 (71.5)	SmC	164.9 (7.91) / 163.3 (7.26)	I

[a] Cr=crystalline, SmC=smectic C and N=nematic phase, I=isotropics.
[b] Observed by microscope.

thermographs were carried out on a Mettler DSC 821 and calibrated with a pure indium sample. All phase transitions are determined by a scan rate of 10.0°/min. Optical polarized microscopy was carried out on a Zeiss AxiaPlan equipped with a hot stage system of Mettler FP90/FP82HT. Elemental analysis for carbon, hydrogen, and nitrogen were conducted on a Heraeus Vario EL-III elemental analyzer at National Taiwan University. All compounds of 4-alkoxybenzaldehydes, 4-alkoxy-2-hydroxy benzaldehydes, 2-{[1-(4-alkoxy phenyl)-methylidene]amino}-4-nitrophenols, 2-(4-alkoxyxyphenyl)-5-nitro-benzoxazoles, and 2-(4-alkoxyphenyl) benzoxazol-5-ylamines were prepared by similar procedures.[6a]

4.1.1. 4-Dodecyloxybenzaldehyde (n=12). White solids; yield 65%. ^{1}H NMR ($CDCl_3$): δ 0.84 (t, *J*=5.93 Hz, $-CH_3$, 3H), 1.23 (m, $-CH_2$, 18H), 1.70–1.84 (m, $-OCH_2CH_2$, 2H), 4.00 (t, *J*=6.51 Hz, $-OCH_2$, 2H), 6.92–6.97 (m, Ar–H, 2H), 7.75–7.80 (m, Ar–H, 2H), 9.83 (s, –CHO, 1H). ^{13}C NMR ($CDCl_3$): δ 14.04, 22.61, 25.88, 28.97, 29.27, 29.48, 29.51, 29.57, 31.84, 68.32, 114.64, 129.63, 131.88, 164.18, 190.68.

*4.1.2. 2-{[1-(4-Dodecyloxyphenyl)-methylidene]amino}-4-nitrophenol (**5**; n=12).* The solution of 4-dodecyloxybenzaldehyde (5.0 g, 0.017 mol) dissolved in 100 mL dry C_2H_5OH with a few drops CH_3COOH added was added 2-amino-4-nitrophenol (2.66 g, 0.017 mol), and the solution was refluxed for 12 h under nitrogen atmosphere. The solution was cooled and the solids were collected. The products isolated as yellow solids were obtained by recrystallization from C_2H_5OH. Yield 90%. ^{1}H NMR ($CDCl_3$): δ 0.86 (t, *J*=6.71 Hz, $-CH_3$, 3H), 1.25 (m, $-CH_2$, 18H), 1.73–1.84 (m, $-OCH_2CH_2$, 2H), 4.03 (t, *J*=6.48 Hz, $-OCH_2$, 2H), 6.96–7.07 (m, Ar–H, 3H), 7.87 (d, *J*=8.73 Hz, Ar–H, 2H), 8.09 (dd, *J*=2.54 Hz, 8.89 Hz, Ar–H, 1H), 8.19 (d, *J*=2.55 Hz, Ar–H, 1H), 8.69 (s, Ar-CHN, 1H). ^{13}C NMR ($CDCl_3$): δ 14.11, 22.68, 25.97, 29.09, 29.34, 29.56,

Table 4
Phase transitions and ehthalpies[a] of compounds **1a–h–M** (M=Cu, Ni, Pd, Zn, Co)

Compound	n	m	Heating	Cooling
1a-Cu	1	1	Cr 284.6 (20.5) N 304.2 (0.42) I_d	I_d 275.8[b] N 144.2[b] Cr
1b-Cu	1	12	Cr 208.3 (37.0) N 255.5 (0.40) I	I 221.7 (0.32) N 156.4[b] Cr
1c-Cu	8	1	Cr 185.1 (68.1) N 255.6 (1.03) I	I 236.4 (0.34) N 85.3[b] Cr
1d-Cu	12	1	Cr 176.8 (63.0) N 227.3 (0.97) I	I 222.1 (0.78) N 80.1[b] Cr
1e-Cu	12	4	Cr 154.4 (59.0) N 223.1 (1.00) I	I 219.8 (0.94) N 83.3 (8.01) Cr
1f-Cu	12	8	Cr 193.4 (53.4) N 212.6 (1.66) I	I 209.3 (1.62) N 190.7 (1.55) SmC 145.4 (37.8) Cr
1g-Cu	12	12	Cr 162.3 (56.1) SmC 197.2 (10.6) I	I 195.6 (10.3) SmC 124.3 (48.1) Cr
1h-Cu	12	16	Cr 151.6 (65.9) SmC 192.6 (13.2) I	I 191.5 (11.4) SmC 114.0 (54.0) Cr
1f-Ni	12	8	Cr 126.5 (12.1) SmC 184.8 (5.57) N 197.3[b] I	I 193.5[b] N 177.0 (5.48) SmC 85.7[b] Cr
1g-Ni	12	12	Cr 104.1 (57.0) SmC 174.2 (8.08) I	I 165.5 (4.72) SmC 86.1[b] Cr
1f-Pd	12	8	Cr 161.3 (4.24) SmC 200.0 (1.90) N 228.8 (1.25) I	I 228.0 (1.07) N 198.7 (1.62) SmC 144.5 (11.2) Cr
1g-Pd	12	12	Cr 160.2 (7.12) SmC 214.6 (2.82) N 224.4 (0.47) I	I 218.5 (0.46) N 209.2 (2.60) SmC 102.5 (32.0) Cr
1g-Zn	12	12	Cr 200.2 (48.9) I	I 189.9 (48.7) Cr
1g-Co	12	12	Cr 198.8 (37.1) I	I 182.7 (36.3) Cr

[a] Cr=crystalline, SmC=smectic C and N=nematic phase, I=isotropics.
[b] Observed by microscope

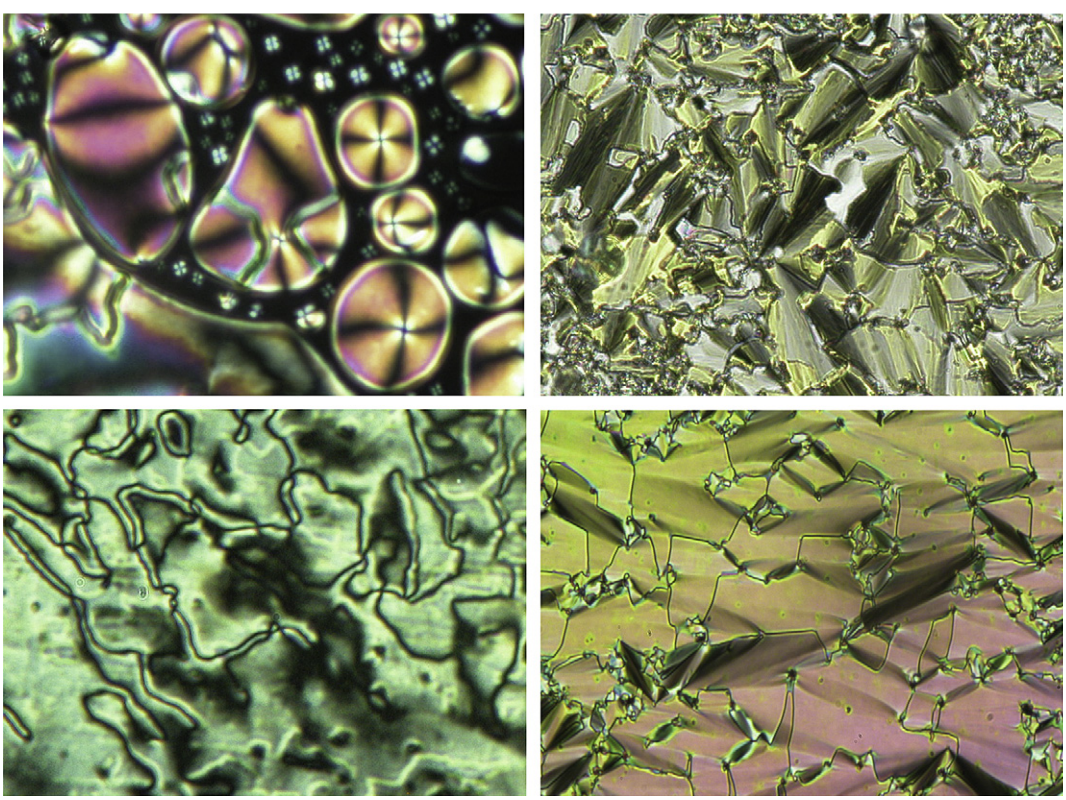

Fig. 6. The optical textures. N phase at 176.0 °C (top left) and SmC phase at 160.0 °C (top right) by **2g**, and N phase at 220 °C (bottom left) and SmC phase at 200 °C (bottom right) by **1g–Pd**.

Table 5
Powder XRD diffraction data for compounds **2g**–**h** and **1g**–**h**–**M**

Compds	Mesophase (temp/°C)	*d*-Spacing (Å)	Miller index	Molecular length (Å)
2g (*n*=12, *m*=12)	SmC at 150 °C	38.2	001	47.1
		4.60	Halo	
2h (*n*=12, *m*=16)	SmC at 148 °C	39.8	001	52.0
		19.9	002	
		4.60	Halo	
1g–**Cu** (*n*=12, *m*=12)	SmC at 182 °C	34.3	001	52.9
		17.2	002	
		4.60	Halo	
1h–**Cu** (*n*=12, *m*=16)	SmC at 188 °C	36.9	001	53.2
		18.5	002	
		4.60	Halo	
1g–**Pd** (*n*=12, *m*=12)	SmC at 206 °C	34.8	001	54.0
		17.4	002	
		4.60	Halo	

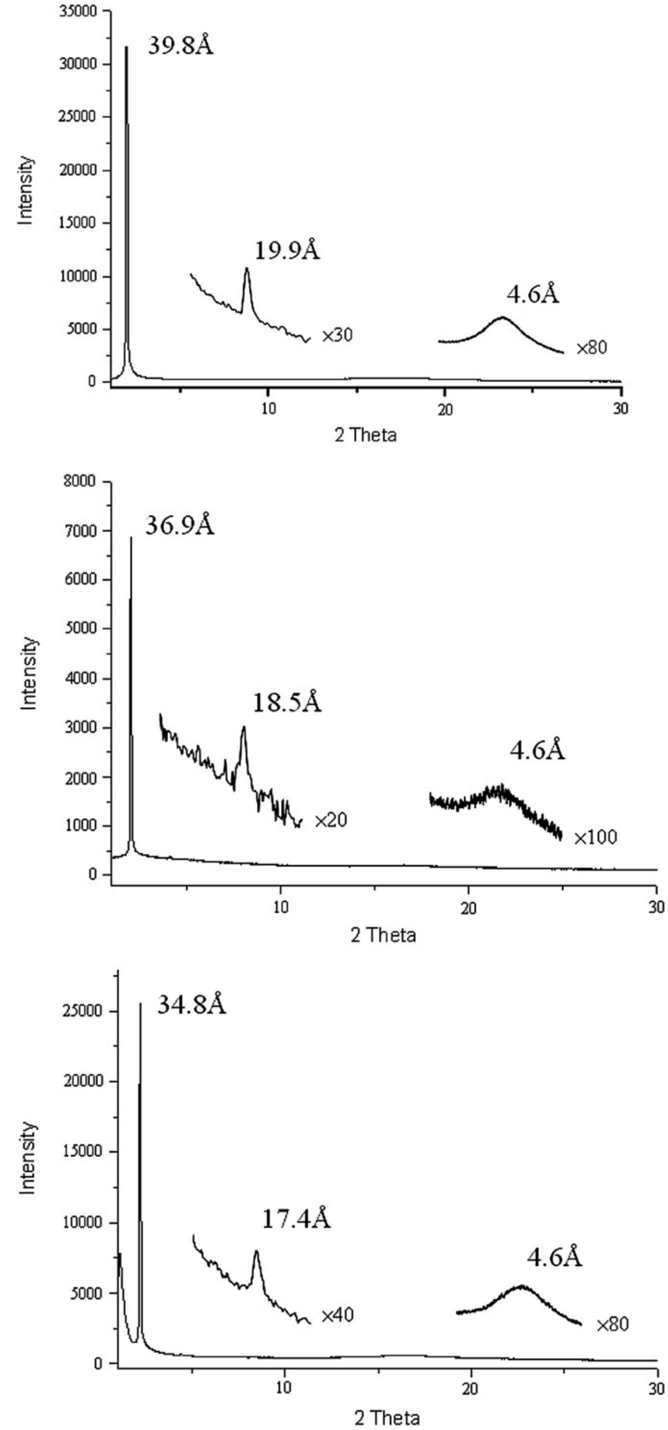

Fig. 7. Powder XRD diffraction plots of **2h** at 148 °C (top left), **1h**–**Cu** at 188 °C and **1g**–**Pd** at 200 °C (bottom).

29.63, 31.90, 68.38, 111.77, 114.63, 115.01, 123.98, 127.64, 131.29, 135.97, 141.18, 157.62, 159.72, 163.06.

*4.1.3. 2-(4-Dodecyloxyphenyl)-5-nitrobenzoxazole (**4**; n=12).* The mixture of 2-{[1-(4-dodecyloxy-phenyl)-methylidene]-amino}-4-nitrophenol (7.0 g, 0.016 mol) dissolved in 200 mL of $CHCl_3$ and $Pb(OAc)_4$ (9.74 g, 0.021 mol) was refluxed for 4 h. The solution was extracted with 100 mL of CH_2Cl_2/H_2O, and the organic layers were combined and dried over $MgSO_4$. The solution was concentrated and the brown solids. The residue was purified by column chromatography (silica gel) eluting with hexane/EA (20/1). The products isolated as pale solids were obtained by recrystallization from CH_2Cl_2/CH_3OH. Yield 83%. ^{1}H NMR ($CDCl_3$): δ 0.86 (t, *J*=5.84 Hz, $-CH_3$, 3H), 1.25 (m, $-CH_2$, 18H), 1.74–1.88 (m, $-OCH_2CH_2$, 2H), 4.03 (t, *J*=6.48 Hz, $-OCH_2$, 2H), 6.99–7.04 (m, Ar–H, 2H), 7.61 (d, *J*=8.90 Hz, Ar–H, 1H), 8.15–8.19 (m, Ar–H, 2H), 8.26 (dd, *J*=2.30 Hz, 8.92 Hz, Ar–H, 1H), 8.57 (d, *J*=2.22 Hz, Ar–H, 1H). ^{13}C NMR ($CDCl_3$): δ 14.11, 22.67, 25.96, 29.07, 29.34, 29.56, 29.62, 31.90, 68.35, 110.35, 115.02, 115.68, 117.97, 120.60, 129.87, 142.81, 145.26, 154.24, 162.80, 166.17.

*4.1.4. 2-(4-Dodecyloxyphenyl)benzoxazol-5-ylamine (**3**; n=12).* The mixture of 2-(4-dodecyloxy-phenyl)-5-nitro-benzoxazole (5.0 g, 0.012 mol) and Pd/C (0.125 g, 0.001 mol) dissolved in 100 mL abs C_2H_5OH was refluxed for 20 min. To this solution, N_2H_4 (0.649 g, 0.013 mol) was added and then refluxed for 6 h. The solids were filtered off and the solution was concentrated to dryness. The product isolated as white solids was obtained after recrystallization from C_2H_5OH. Yield 80%. ^{1}H NMR ($CDCl_3$): δ 0.86 (t, *J*=5.84 Hz, $-CH_3$, 3H), 1.24 (m, $-CH_2$, 18H), 1.75–1.82 (m, $-OCH_2CH_2$, 2H), 3.69 (br, $-NH_2$, 2H), 4.00 (t, *J*=6.06 Hz, $-OCH_2$, 2H), 6.64 (dd, *J*=2.20 Hz, 8.52 Hz, Ar–H, 1H), 6.95–6.99 (m, Ar–H, 3H), 7.29 (d, *J*=8.46 Hz, Ar–H, 1H), 8.09–8.13 (m, Ar–H, 2H). ^{13}C NMR ($CDCl_3$): δ 14.09, 22.66, 25.97, 29.13, 29.33, 29.56, 29.62, 31.89, 68.19, 104.83, 110.35, 113.04, 114.73, 119.64, 129.14, 143.30, 143.68, 144.66, 161.74, 163.67.

4.1.5. 4-Dodecyloxy-2-hydroxybenzaldehyde (m=12). White solid; yield 65%. ^{1}H NMR ($CDCl_3$): δ 0.86 (t, *J*=5.84 Hz, $-CH_3$, 3H), 1.25 (m, $-CH_2$, 18H), 1.77 (m, $-OCH_2CH_2$, 2H), 3.98 (t, *J*=6.00 Hz, $-OCH_2$, 2H), 6.39 (m, Ar–H, 1H), 6.48–6.53 (m, Ar–H, 1H), 7.39 (d, *J*=8.46 Hz, Ar–H, 1H), 9.68 (s, –CHO, 1H), 11.47 (s, Ar–OH, 1H). ^{13}C NMR ($CDCl_3$): δ 14.11, 22.67, 25.89, 28.89, 29.32, 29.61, 31.89, 68.58, 101.00, 108.77, 114.96, 135.18, 164.50, 166.45, 194.29.

*4.1.6. 5-Dodecyloxy-2-{[2-(4-dodecyloxyphenyl)benzoxazol-5-ylimino] methyl}phenol **2g**.* Under the nitrogen atmosphere, the mixture of 4-dodecyloxy-2-hydroxybenzaldehyde (1.0 g, 0.003 mol), 2-(4-dodecyloxy-phenyl)-benzoxazol-5-ylamine (1.287 g, 0.003 mol), and acetic acid (0.5 mL) was gently refluxed for 12 h. The solution was cooled and the solids were collected. The product isolated as yellow solids were obtained after recrystallization from CH_2Cl_2/MeOH. Yield 79%. ^{1}H NMR ($CDCl_3$): δ 0.88 (t, *J*=6.56 Hz, $-CH_3$, 6H), 1.27 (m, $-CH_2$, 36H), 1.78–1.83 (m, $-OCH_2CH_2$, 4H), 4.00 (t, *J*=6.58 Hz, $-OCH_2$, 2H), 4.04 (t, *J*=6.51 Hz, $-OCH_2$, 2H), 6.49–6.53 (m, Ar–H, 2H), 7.02 (d, *J*=8.73 Hz, Ar–H, 2H), 7.24 (d, *J*=8.53 Hz, Ar–H, 1H), 7.29 (d, *J*=8.44 Hz, Ar–H, 1H), 7.54 (d, *J*=8.51 Hz, Ar–H, 1H), 7.58 (s, Ar–H, 1H), 8.17 (d, J=8.71 Hz, Ar–H, 2H), 8.56 (s, –NCH, 1H). ^{13}C NMR ($CDCl_3$): δ 14.46, 23.04, 26.34, 29.43, 29.50, 29.70, 29.72, 29.91, 29.94, 29.99, 30.01, 32.27, 68.64, 101.94, 108.06, 110.94, 110.97, 113.27, 115.24, 119.38, 119.52, 129.80, 133.94, 143.68, 145.99, 149.71, 161.78, 162.50, 164.05, 164.76. MS (FAB): calcd for MH^+ $C_{44}H_{63}N_2O_4$: 684.0. Found: 684.5. Anal. Calcd for $C_{44}H_{62}N_2O_4$: C, 77.38; H, 9.15; N, 4.10. Found: C, 77.03; H, 9.09; N, 4.11. IR (KBr): 3066, 2919, 2850, 1631, 1603, 1500, 1470, 1248, 827, 807 cm^{-1}.

4.1.7. 5-Methoxy-2-{[2-(4-methoxyphenyl)benzoxazol-5-ylimino] methyl}phenol ***2a***. Yellow solid; 81%. ^{1}H NMR ($CDCl_3$): δ 3.83 (s, –CH_3, 3H), 3.88 (s, –CH_3, 3H), 6.48–6.51 (m, Ar–H, 2H), 7.01 (d, J=8.87 Hz, Ar–H, 2H), 7.22 (dd, J=1.99 Hz, 8.51 Hz, Ar–H, 1H), 7.28 (d, J=8.40 Hz, Ar–H, 1H), 7.54 (d, J=8.51 Hz, Ar–H, 1H), 7.58 (s, Ar–H, 1H), 8.17 (d, J=8.71 Hz, Ar–H, 2H), 8.56 (s, N=CH, 1H).^{13}C NMR ($CDCl_3$): δ 55.47, 101.06, 107.15, 110.63, 113.14, 114.39, 119.11, 119.44, 129.46, 133.56, 143.26, 145.77, 149.34, 161.51, 162.47, 163.67, 163.94, 164.29. MS (FAB): calcd for MH^+ $C_{22}H_{19}N_2O_4$: 375.4. Found: 375.2. Anal. Calcd for $C_{22}H_{18}N_2O_4$: C, 70.58; H, 4.85; N, 7.48. Found: C, 70.47; H, 4.79; N, 7.46. IR (KBr): 1628, 1605, 1505, 1259, 1167, 1142, 1026, 831, 805 cm^{-1}.

4.1.8. 5-Dodecyloxy-2-{[2-(4-methoxyphenyl)benzoxazol-5-ylimino] methyl}phenol ***2b***. Yellow solid; 83%. ^{1}H NMR ($CDCl_3$): δ 0.86 (t, J=6.69 Hz, –CH_3, 3H), 1.24 (m, –CH_2, 18H), 1.76–1.79 (m, –OCH_2CH_2, 2H), 3.87 (s, –OCH_3, 3H), 3.97 (s, –OCH_2, 2H), 6.47–6.52 (m, Ar–H, 2H), 7.01 (d, J=8.81 Hz, Ar–H, 2H), 7.23 (s, Ar–H, 1H), 7.27 (s, Ar–H, 1H), 7.51 (d, J=8.29 Hz, Ar–H, 1H), 7.56 (s, Ar–H, 1H), 8.15 (d, J=2.05 Hz, Ar–H, 1H), 8.17 (s, Ar–H, 1H), 8.53 (s, –NCH, 1H). ^{13}C NMR ($CDCl_3$): δ 14.12, 22.68, 25.96, 29.05, 29.35, 29.55, 29.58, 29.62, 29.65, 31.90, 55.45, 68.30, 101.53, 107.74, 110.58, 110.65, 112.75, 114.38, 119.01, 119.39, 129.46, 133.65, 143.26, 149.34, 161.36, 162.47, 163.76, 164.29. MS (FAB): calcd for MH^+ $C_{33}H_{41}N_2O_4$: 529.7. Found: 529.5. Anal. Calcd for $C_{33}H_{40}N_2O_4$: C, 74.97; H, 7.63; N, 5.30. Found: C, 74.80; H, 7.65; N, 5.27. IR (KBr): 3607, 2918, 2851, 1630, 1607, 1503, 1253, 829, 805 cm^{-1}.

4.1.9. 5-Methoxy-2-{[2-(4-octyloxyphenyl)benzoxazol-5-ylimino] methyl}phenol ***2c***. Yellow solid; 88%. ^{1}H NMR ($CDCl_3$): δ 0.89 (t, J=6.76 Hz, –CH_3, 3H), 1.30–1.34 (m, –CH_2, 10H), 1.78–1.83 (m, –OCH_2CH_2, 2H), 3.84 (s, –OCH_3, 3H), 4.02 (t, J=6.53 Hz, –OCH_2, 2H), 6.49–6.52 (m, Ar–H, 2H), 7.00 (d, J=8.82 Hz, Ar–H, 2H), 7.22 (dd, J=2.05 Hz, 8.53 Hz, Ar–H, 1H), 7.29 (d, J=8.49 Hz, Ar–H, 1H), 7.52 (d, J=8.50 Hz, Ar–H, 1H), 7.57 (d, J=1.92 Hz, Ar–H, 1H), 8.16 (d, J=8.80 Hz, Ar–H, 2H), 8.55 (s, –NCH, 1H). ^{13}C NMR($CDCl_3$): δ 14.42, 22.98, 26.34, 29.49, 29.56, 29.67, 32.14, 55.79, 68.63, 101.46, 107.46, 110.92, 110.96, 113.53, 115.22, 119.36, 119.52, 129.78, 133.90, 143.67, 146.09, 149.70, 161.77, 162.48, 164.05, 164.30, 164.72. MS (FAB): calcd for MH^+ $C_{29}H_{33}N_2O_4$: 473.6. Found: 473.3. Anal. Calcd for $C_{33}H_{40}N_2O_4$: C, 73.70; H, 6.83; N, 5.93. Found: C, 73.66; H, 6.89; N, 5.91. IR (KBr): 3062, 2929, 2855, 1629, 1601, 1500, 1254, 1172, 1136 cm^{-1}.

4.1.10. 5-Methoxy-2-{[2-(4-dodecyloxyphenyl)benzoxazol-5-ylimino]methyl}phenol ***2d***. Yellow solid; 80%. ^{1}H NMR ($CDCl_3$): δ 0.86 (t, J=6.69 Hz, –CH_3, 3H), 1.24 (m, –CH_2, 18H), 1.76–1.79 (m, –OCH_2CH_2, 2H), 3.87 (s, –OCH_3, 3H), 3.97 (t, J=6.54 Hz, –OCH_2, 2H), 6.47–6.52 (m, Ar–H, 2H), 7.01 (d, J=8.81 Hz, Ar–H, 2H), 7.23 (s, Ar–H, 2H), 7.27 (s, Ar–H, 2H), 7.51 (d, J=8.29 Hz, Ar–H, 2H), 8.15–8.17 (m, Ar–H, 2H), 8.53 (s, –NCH, 1H). ^{13}C NMR ($CDCl_3$): δ 14.43, 23.01, 26.34, 29.50, 29.68, 29.72, 29.90, 29.93, 29.97, 29.99, 32.25, 55.77, 68.62, 101.46, 107.44, 110.90, 110.97, 113.53, 115.21, 119.34, 119.53, 129.77, 133.89, 143.67, 146.07, 149.70, 161.73, 162.47, 164.05, 164.30, 164.71. MS (FAB): calcd for MH^+ $C_{33}H_{41}N_2O_4$: 529.7. Found: 529.4. Anal. Calcd for $C_{33}H_{40}N_2O_4$: C, 74.97; H, 7.63; N, 5.30. Found: C, 74.80; H, 7.77; N, 5.27. IR (KBr): 3064, 2917, 2850, 1631, 1609, 1502, 1254, 826, 808 cm^{-1}.

4.1.11. 5-Butoxy-2-{[2-(4-dodecyloxyphenyl)benzoxazol-5-ylimino] methyl}phenol ***2e***. Yellow solid; yield 86%. ^{1}H NMR ($CDCl_3$): δ 0.89 (t, J=6.69 Hz, –CH_3, 3H), 0.99 (t, J=7.37 Hz, –CH_3, 3H), 1.27 (m, –CH_2, 20H), 1.77–1.82 (m, –OCH_2CH_2, 4H), 3.98–4.02 (m, –OCH_2, 4H), 6.48–6.50 (m, Ar–H, 2H), 7.00 (d, J=8.76 Hz, Ar–H, 2H), 7.21 (d, J=7.02 Hz, Ar–H, 1H), 7.26 (d, J=7.85 Hz, Ar–H, 1H), 7.50 (d, J=8.52 Hz, Ar–H, 1H), 7.56 (s, Ar–H, 1H), 8.15 (d, J=8.70 Hz, Ar–H, 2H), 8.53 (s, –NCH, 1H). ^{13}C NMR ($CDCl_3$): δ 14.14, 14.44, 19.53, 23.01, 26.33, 29.49, 29.68, 29.72, 29.90, 29.93, 29.97, 29.99, 30.65, 31.46, 32.25, 68.25, 68.59, 101.89, 107.87, 110.87, 110.92, 113.33, 115.17, 119.32, 119.50, 129.74, 133.83, 143.63, 146.07, 149.64, 161.69, 162.43, 163.89, 164.00, 164.65. MS (FAB): calcd for MH^+ $C_{36}H_{47}N_2O_4$: 571.8. Found: 571.4. Anal. Calcd for $C_{36}H_{46}N_2O_4$: C, 75.76; H, 8.12; N, 4.91. Found: C, 75.57; H, 8.16; N, 4.88. IR (KBr): 3064, 2918, 2851, 1632, 1605, 1503, 1474, 1250, 829, 807 cm^{-1}.

4.1.12. 5-Octyloxy-2-{[2-(4-dodecyloxyphenyl)benzoxazol-5-ylimino]methyl}phenol ***2f***. Yellow solid; yield 84%. ^{1}H NMR ($CDCl_3$): δ 0.88 (t, J=5.89 Hz, –CH_3, 6H), 1.27 (m, –CH_2, 28H), 1.77–1.82 (m, –OCH_2CH_2, 4H), 3.97–4.02 (m, –OCH_2, 4H), 6.47–6.49 (m, Ar–H, 2H), 6.99 (d, J=8.80 Hz, Ar–H, 2H), 7.21 (d, J=8.51 Hz, Ar–H, 1H), 7.26 (d, J=8.41 Hz, Ar–H, 1H), 7.50 (d, J=8.55 Hz, Ar–H, 1H), 7.55 (d, J=1.80 Hz, Ar–H, 1H), 8.15 (d, J=8.76 Hz, Ar–H, 2H), 8.53 (s, –NCH, 1H). ^{13}C NMR ($CDCl_3$): δ 14.43, 14.44, 22.99, 23.02, 26.33, 29.42, 29.49, 29.56, 29.68, 29.72, 29.90, 29.93, 29.97, 30.00, 32.14, 32.25, 68.58, 101.89, 107.88, 110.88, 110.91, 113.32, 115.17, 119.34, 119.49, 129.75, 133.83, 143.62, 146.07, 149.63, 161.70, 162.44, 163.89, 164.00, 164.66. MS (FAB): calcd for MH^+ $C_{40}H_{55}N_2O_4$: 627.9. Found: 627.5. Anal. Calcd for $C_{40}H_{54}N_2O_4$: C, 76.64; H, 8.68; N, 4.47. Found: C, 76.56; H, 8.72; N, 4.42. IR (KBr): 3064, 2919, 2851, 1631, 1604, 1502, 1474, 1252, 828, 808 cm^{-1}.

4.1.13. 5-Hexadecyloxy-2-{[2-(4-dodecyloxyphenyl)benzoxazol-5-ylimino]methyl}phenol ***2h***. Yellow solid; yield 88%. ^{1}H NMR ($CDCl_3$): δ 0.89 (t, J=6.29 Hz, –CH_3, 6H), 1.27 (m, –CH_2, 44H), 1.80–1.83 (m, –OCH_2CH_2, 4H), 3.99–4.05 (m, –OCH_2, 4H), 6.49 (m, Ar–H, 2H), 6.98 (m, Ar–H, 2H), 7.23 (s, Ar–H, 1H), 7.29 (s, Ar–H, 1H), 7.52 (d, J=7.99 Hz, Ar–H, 1H), 7.58 (s, Ar–H, 1H), 8.17 (d, J=8.52 Hz, Ar–H, 2H), 8.56 (s, –NCH, 1H). ^{13}C NMR ($CDCl_3$): δ 14.46, 21.56, 23.07, 26.41, 29.52, 29.58, 29.74, 29.77, 29.96, 29.99, 30.03, 30.05, 30.09, 30.76, 32.32, 34.63, 68.71, 68.73, 108.04, 110.95, 111.07, 115.21, 115.32, 119.44, 119.70, 125.89, 129.86, 133.95, 136.29, 143.80, 146.30, 149.80, 161.84, 162.58, 164.00, 164.79. MS (FAB): calcd for MH^+ $C_{48}H_{71}N_2O_4$: 740.1. Found: 740.5. Anal. Calcd for $C_{48}H_{70}N_2O_4$: C, 78.00; H, 9.55; N, 3.79. Found: C, 77.99; H, 9.62; N, 3.73. IR (KBr): 3064, 2918, 2850, 1633, 1605, 1505, 1472, 1254, 829 cm^{-1}.

*4.1.14. Bis[5-dodecyloxy-2-{[2-(4-dodecyloxyphenyl)benzoxazol-5-ylimino]methyl}phenol] copper (**1g–Cu**; n=12, m=12).* The mixture of 5-dodecyloxy-2-{[2-(4-dodecyloxyphenyl)benzoxazol-5-ylimino] methyl}phenol (0.1 g, 0.01 mmol) and copper(II) acetate hydrate (0.015 g, 0.007 mmol) was dissolved in 20 mL of C_2H_5OH, and the solution was gently refluxed for 2 h. The solution was cooled and the solids were collected. The products isolated as gray to green solid were obtained by recrystallization from CH_2Cl_2/CH_3OH. IR (KBr): 2923, 2852, 1612, 1501, 1469, 1252, 835, 812 cm^{-1}. MS (FAB): calcd for MH^+ $C_{88}H_{123}N_4O_8Cu$: 1428.5. Found: 1428.6. Anal. Calcd for $C_{88}H_{122}N_4O_8Cu$: C, 74.04; H, 8.61; N, 3.92. Found: C, 73.60; H, 8.72; N, 3.75.

*4.1.15. Bis[5-methoxy-2-{[2-(4-methoxyphenyl)benzoxazol-5-ylimino]methyl}phenol]copper (**1a–Cu**; n=1, m=1).* Green solid, IR

(KBr): 1611, 1504, 1259, 1228, 1168, 1139, 1025, 829 cm^{-1}. MS (FAB): calcd for MH$^+$ $C_{44}H_{35}N_4O_8Cu$: 811.3. Found: 811.2.

*4.1.16. Bis[5-dodecyloxy-2-{[2-(4-methoxyphenyl)benzoxazol-5-ylimino]methyl}phenol]copper (**1b**–**Cu**; n=1, m=12).* Green solid, IR (KBr): 2924, 2853, 1610, 1502, 1468, 1253, 836 cm^{-1}. MS (FAB): calcd for MH$^+$ $C_{66}H_{79}N_4O_8Cu$: 1119.9. Found: 1119.8. Anal. Calcd for $C_{66}H_{78}N_4O_8Cu$: C, 70.85; H, 7.03; N, 5.01. Found: C, 70.39; H, 7.06; N, 4.96.

*4.1.17. Bis[5-methoxy-2-{[2-(4-octyloxyphenyl)benzoxazol-5-ylimino]methyl}phenol]copper (**1c**–**Cu**; n=8, m=1).* Green solid, IR (KBr): 2925, 2853, 1607, 1500, 1466, 1254, 1221, 835 cm^{-1}. MS (FAB): calcd for MH$^+$ $C_{58}H_{63}N_4O_8Cu$: 1007.7. Found: 1007.3. Anal. Calcd for $C_{58}H_{62}N_4O_8Cu$: C, 69.20; H, 6.21; N, 5.57. Found: C, 68.79; H, 6.19; N, 5.41.

*4.1.18. Bis[5-methoxy-2-{[2-(4-dodecyloxyphenyl)benzoxazol-5-ylimino]methyl}phenol]copper (**1d**–**Cu**; n=12, m=1).* Green solid, IR (KBr): 2922, 2852, 1610, 1594, 1499, 1468, 1254, 1221, 836 cm^{-1}. MS (FAB): calcd for MH$^+$ $C_{66}H_{79}N_4O_8Cu$: 1119.9. Found: 1119.8. Anal. Calcd for $C_{66}H_{78}N_4O_8Cu$: C, 70.85; H, 7.03; N, 5.01. Found: C, 70.39; H, 7.06; N, 4.96.

*4.1.19. Bis[5-butoxy-2-{[2-(4-dodecyloxyphenyl)benzoxazol-5-ylimino]methyl}phenol]copper (**1e**–**Cu**; n=12, m=4).* Green solid, IR (KBr): 2921, 2852, 1593, 1499, 1471, 1429, 1254, 1222 cm^{-1}. MS (FAB): calcd for MH$^+$ $C_{72}H_{91}N_4O_8Cu$: 1204.1. Found: 1204.5. Anal. Calcd for $C_{72}H_{90}N_4O_8Cu$: C, 71.88; H, 7.54; N, 4.66. Found: C, 71.46; H, 7.42; N, 4.43.

*4.1.20. Bis[5-octyloxy-2-{[2-(4-dodecyloxyphenyl)benzoxazol-5-ylimino]methyl}phenol]copper (**1f**–**Cu**; n=12, m=8).* Green solid, IR (KBr): 2926, 2853, 1611, 1500, 1469, 1253, 835, 812 cm^{-1}. MS (FAB): calcd for MH$^+$ $C_{80}H_{107}N_4O_8Cu$: 1316.3. Found: 1316.6. Anal. Calcd for $C_{80}H_{106}N_4O_8Cu$: C, 73.05; H, 8.12; N, 4.26. Found: C, 72.98; H, 8.08; N, 4.17.

*4.1.21. Bis[5-hexadecyloxy-2-{[2-(4-dodecyloxyphenyl)benzoxazol-5-ylimino]methyl}phenol] copper (**1h**–**Cu**; n=12, m=16).* Green solid, IR (KBr): 2921, 2851, 1612, 1501, 1469, 1254 cm^{-1}. MS (FAB): calcd for MH$^+$ $C_{96}H_{139}N_4O_8Cu$: 1539.7. Found: 1539.9. Anal. Calcd for $C_{96}H_{138}N_4O_8Cu$: C, 74.89; H, 9.03; N, 3.64. Found: C, 73.78; H, 9.04; N, 3.54.

*4.1.22. Bis[5-octyloxy-2-{[2-(4-dodecyloxyphenyl)benzoxazol-5-ylimino]methyl}phenol]nickel (**1f**–**Ni**; n=12, m=8).* Yellow solid, IR (KBr): 2922, 2852, 1604, 1500, 1468, 1253, 1211, 1135, 836 cm^{-1}. MS (FAB): calcd for MH$^+$ $C_{80}H_{107}N_4O_8Ni$: 1359.1. Found: 1359.7. Anal. Calcd for $C_{80}H_{106}N_4NiO_8$: C, 73.32; H, 8.15; N, 4.28. Found: C, 72.99; H, 8.30; N, 4.02.

*4.1.23. Bis[5-dodecyloxy-2-{[2-(4-dodecyloxyphenyl)benzoxazol-5-ylimino]methyl}phenol] nickel (**1g**–**Ni**; n=12, m=12).* Yellow solid, IR (KBr): 2919, 2851, 1607, 1503, 1472, 1253, 831, 807 cm^{-1}. MS (FAB): calcd for MH$^+$ $C_{88}H_{123}N_4O_8Ni$: 1423.6. Found: 1423.7.

*4.1.24. Bis[5-octyloxy-2-{[2-(4-dodecyloxyphenyl)benzoxazol-5-ylimino]methyl}phenol]palladium (**1f**–**Pd**; n=12, m=8).* Light orange solid, IR (KBr): 2922, 2852, 1604, 1500, 1468, 1253, 1211, 1135, 836 cm^{-1}. MS (FAB): calcd for MH$^+$ $C_{80}H_{107}N_4O_8Pd$: 1359.1. Found: 1359.7. Anal. Calcd for $C_{80}H_{106}N_4O_8Pd$: C, 70.75; H, 7.87; N, 4.13. Found: C, 71.15; H, 8.13; N, 4.11.

*4.1.25. Bis[5-dodecyloxy-2-{[2-(4-dodecyloxyphenyl)benzoxazol-5-ylimino]methyl}phenol] palladium (**1g**–**Pd**; n=12, m=12).* Orange solid, IR (KBr): 2925, 2854, 1606, 1523, 1499, 1469, 1253, 833, 811 cm^{-1}. MS (FAB): calcd for MH$^+$ $C_{88}H_{123}N_4O_8Pd$: 1471.4. Found: 1471.2. Anal. Calcd for $C_{88}H_{122}N_4O_8Pd$: C, 71.88; H, 8.36; N, 3.81. Found: C, 71.89; H, 8.51; N, 3.72.

*4.1.26. Bis[5-dodecyloxy-2-{[2-(4-dodecyloxyphenyl)benzoxazol-5-ylimino]methyl}phenol]zinc (**1g**–**Zn**; n=12, m=12).* Pale-yellow solid, IR (KBr): 2922, 2851, 1612, 1500, 1430, 1253, 1222, 834, 804 cm^{-1}. MS (FAB): calcd for MH$^+$ $C_{88}H_{123}N_4O_8Zn$: 1430.3. Found: 1430.8. Anal. Calcd for $C_{88}H_{122}N_4O_8Zn$: C, 73.95; H, 8.60; N, 3.92. Found: C, 73.59; H, 8.67; N, 3.97.

*4.1.27. Bis[5-dodecyloxy-2-{[2-(4-dodecyloxyphenyl)benzoxazol-5-ylimino]methyl}phenol]cobalt (**1g**–**Co**; n=12, m=12).* Brown solid, IR (KBr): 2925, 2853, 1606, 1500, 1469, 1423, 1250, 837, 808 cm^{-1}. MS (FAB): calcd for MH$^+$ $C_{88}H_{123}N_4O_8Co$: 1423.9. Found: 1423.8. Anal. Calcd for $C_{88}H_{122}CoN_4O_8$: C, 74.28; H, 8.64; N, 3.94. Found: C, 74.17; H, 8.75; N, 3.96.

Acknowledgements

We thank the National Science Council of Taiwan, ROC (NSC98-2815-C-008-021-M).

References and notes

1. (a) Porta, B.; Klamsi, J.; Noveron, J. *Curr. Org. Chem.* **2008**, *12*, 1–24; (b) Date, R. W.; Iglesias, E. F.; Rowe, K. E.; Elliott, J. M.; Bruce, D. W. *Dalton Trans.* **2003**, 1914–1931; (c) Gimenez, R.; Lydon, D. P.; Serrano, J. L. *Currr. Opin. Solid State Mater. Sci.* **2002**, *6*, 527–535; (d) Donnio, B.; Bruce, D. W. *Struct. Bonding* **1999**, *95*, 194–242; (e) Hoshino, N. *Coord. Chem. Rev.* **1998**, 77–108; (f) *Inorganic Materials*; Bruce, D. W., Ed.; John Wiley: New York, NY, 1997; (g) Bruce, D. R.; O'Hare, D. *Inorganic Materials*, 2nd ed.; Wiley: New York, NY, 1996; (h) Serrano, J. L. *Metallomesogens: Synthesis, Properties, and Applications*; VCH: Weinheim, 1996; (i) Hudson, S. A.; Maltlis, P. M. *Chem. Rev.* **1993**, *93*, 861–885.
2. (a) Chen, C.-J.; Wu, Y.-C.; Sheu, H.-S.; Lee, G.-H.; Lai, C. K. *Tetrahedron* **2011**, *67*, 114–124; (b) Liao, C. C.; Wang, C. S.; Shen, H. S.; Lai, C. K. *Tetrahedron* **2008**, *64*, 7977–7985; (c) Wang, C. S.; Wang, I. W.; Lai, C. K. *Tetrahedron* **2006**, *62*, 9383–9392; (d) Lai, C. K.; Liu, H. C.; Li, F. J.; Cheng, K. L.; Sheu, H. S. *Liq. Cryst.* **2005**, *32*, 85–94.
3. Gimenez, R.; Oriol, L.; Pinol, M.; Serrano, J. L.; Vinuales, A. I.; Fisher, T.; Stumpe, J. *Helv. Chim. Acta* **2006**, *89*, 304–319.
4. (a) Xu, Y.; Pang, Y. *Dalton Trans.* **2011**, *40*, 1503–1509; (b) Xu, Y.; Pang, Y. *Chem. Commun.* **2011**, 4070–4072; (c) Kim, T. H.; Kim, D. G.; Lee, M.; Lee, T. S. *Tetrahedron* **2010**, *66*, 1667–1672; (d) Shavaleev, N. M.; Scopelliti, R.; Gumy, F.; Bunzli, J. C. G. *Inorg. Chem.* **2009**, *48*, 2908–2918; (e) Shavaleev, N. M.; Scopelliti, R.; Gumy, F.; Bunzli, J. C. G. *Inorg. Chem.* **2009**, *48*, 6178–6191; (f) Tian, Y.; Chen, C. Y.; Yang, C. C.; Young, A. C.; Jang, S. H.; Chen, W. C.; Jen, A. K. Y. *Chem. Mater.* **2008**, *20*, 1977–1987; (g) Klare, J. E.; Tulevski, G. S.; Sugo, K.; Picciotto, A. D.; White, K. A.; Nuckolls, C. *J. Am. Chem. Soc.* **2003**, *125*, 6030–6031; (h) Costa, T. M. H.; Stefani, V.; Gallas, M. R.; Balzaretti, N. M.; Da Jornada, J. A. H. *J. Mater. Chem.* **2001**, *11*, 3377–3381; (i) Ko, C. W.; Tao, Y. T. *Chem. Mater.* **2001**, *13*, 2441–2446; (j) Tanaka, K.; Kumagai, T.; Aoki, H.; Deguchi, M.; Iwata, S. *J. Org. Chem.* **2001**, *66*, 7328–7333.
5. (a) Chen, T. R.; Lee, H. P.; Chen, J. D. *Inorg. Chem.* **2011**, *50*, 3645–3650; (b) Back, D. F.; Oliveira, G. M. d; Ballin, M. A.; Corbellini, V. A. *Inorg. Chim. Acta* **2010**, *363*, 807–812; (c) Chu, Q.; Medvetz, D. A.; Panzner, M. J.; Yang, P. *Dalton Trans.* **2010**, *39*, 5254–5259; (d) Małecki, J. G.; Kruszynski, R.; Jaworska, M.; Lodowski, P.; Mazurak, Z. *J. Organom. Chem.* **2008**, *693*, 1096–1108; (e) Keyes, T. E.; Leane, D.; Forster, R. J.; Coates, C. G.; McGarvey, J. J.; Nieuwenhuyzen, M. N.; Figgemeier, E.; Vos, J. G. *Inorg. Chem.* **2002**, *41*, 5721–5732; (f) Chen, X.; Femia, F. J.; Babich, J. W.; Zubieta, J. *Inorg. Chim. Acta* **2001**, *316*, 33–40.
6. (a) Wang, H. C.; Wang, Y. J.; Hu, H. M.; Lee, G. H.; Lai, C. K. *Tetrahedron* **2008**, *64*, 4939–4948; (b) Caruso, U.; Panunzi, B.; Roviello, A.; Tingoli, M.; Tuzi, A. *Inorg. Chem. Commun.* **2011**, *14*, 46–48.
7. (a) Bhattacharjee, C. R.; Das, G.; Mondal, P.; Prasad, S. K.; Rao, D. S. S. *Inorg. Chem. Commun.* **2011**, *14*, 606–612; (b) Bhattacharjee, C. R.; Das, G.; Goswami, P.; Mondal, P.; Prasad, S. K.; Rao, D. S. S. *Polyhedron* **2011**, *30*, 1040–1047; (c) Binnemans, K. *J. Mater. Chem.* **2009**, *19*, 448–453; (d) Pucci, D.; Aiello, I. ,; Bellusci, A.; Crispini, A.; Ghedini, M.; Deda, M. L. *Eur. J. Inorg. Chem.* **2009**, 4274–4281; (e) Pucci, D.; Aiello, I.; Bellusci, A.; Callipari, G.; Crispini, A.; Ghedini, M. *Mol. Cryst. Liq. Cryst.* **2009**, *500*, 144–154; (f) Ocak, H.; Bilgin-Eran, B.; Tschierske, C.; Baumeisterc, U.; Pelzlc, G. *J. Mater. Chem.* **2009**, *19*, 6995–7001; (g) Rezvani, Z.; Ghanea, M. A.; Nejati, K.; Baghaei, S. A. *Polyhedron* **2009**, *28*, 2913–2918; (h) Kadkin, O. N.; An, J.; Han, H.; Galyametdino, Y. G. *Eur. J. Inorg. Chem.* **2008**, 1682–1688; (i) Yelamaggad, C. Y.; Shashikala, I. S.; Tamilenthi, V. P.; Rao, D. S. S.; Nair, G. G.; Prasad, S. K. *J. Mater. Chem.* **2008**, *18*, 2096–2103; (j) Singh, A. K.; Kumari, S.; Kumar, K. R.; Sridhar, B.; Rao, T. R. *Polyhedron* **2008**, *27*,

181–186; (k) Aiello, I.; Bellusci, A.; Crispini, A.; Ghedini, M.; Pucci, D.; Spataro, T. *Mol. Cryst. Liq. Cryst.* **2008**, *481*, 1–13; (l) Yang, Y.; Driesen, K.; Nockemann, P.; Hecke, K. V.; Meervelt, L. V.; Binnemans, K. *Chem. Mater.* **2006**, *18*, 3698–3704; (m) Rezvani, Z.; Divband, B.; Abbasi, A. R.; Nejati, K. *Polyhedron* **2006**, *25*, 1915–1929; (n) Abe, Y.; Nakabayashi, K.; Matsukawa, N.; Takashima, H.; Iida, M.; Tanase, T.; Sugibayashi, M.; Mukai, H.; Ohta, K. *Inorg. Chim. Acta* **2006**, *359*, 3934–3946; (o) Binnemans, K.; Lodewyckx, K.; Donnio, B.; Guillon, D. *Eur. J. Inorg. Chem.* **2005**, 1506–1513; (p) Paschke, R.; Liebsch, S.; Tschierske, C.; Oakley, M. A.; Sinn, E. *Inorg. Chem.* **2003**, *42*, 8230–8240; (q) Nejati, K.; Rezvani, Z. *New J. Chem.* **2003**, *27*, 1665–1669; (r) Barbera, J.; Giménez, R.; Marcos, M.; Serrano, J. L.; Alonso, P. J.; Martínez, J. I. *Chem. Mater.* **2003**, *15*, 958–964; (s) Ku, S. M.; Wu, C. Y.; Lai, C. K. *J. Chem. Soc., Dalton Trans.* **2000**, 3491–3492; (t) Lai, C. K.; Cahng, C. H.; Tai, C. H. *J. Mater. Chem.* **1998**, *8*, 599–602; (u) Lai, C. K.; Lin, R.; Lu, M. Y.; Kao, K. C. *J. Chem. Soc., Dalton Trans.* **1998**, 1857–1862.

8. (a) Kakegawa, N.; Hoshino, N.; Matsuoka, Y.; Wakabayashi, N.; Nishimura, S.; Yamagishi, A. *Chem. Commun.* **2005**, 2375–2377; (b) Trazska, S. T.; Hsu, H. F.; Swager, T. M. *J. Am. Chem. Soc.* **1999**, *121*, 4518–4519.
9. (a) Siracusa, M. A.; Salerno, L.; Modica, M. N.; Pittala, V.; Romeo, G.; Amato, M. E.; Nowak, M.; Bojarski, A. J.; Mereghetti, I.; Cagnotto, A.; Mennini, T. *J. Med. Chem.* **2008**, *51*, 4529–4538; (b) Hart, A.; Karan, C.; Rodrigues, W.; Miller, B. L. *J. Org. Chem.* **2001**, *66*, 881–996; (c) So, Y. H.; Zaleski, J. M.; Murlick, C.; Ellaboudy, A. *Macromolecules* **1996**, *29*, 2783–2796.
10. Abou-Zied, O. K.; Jimenez, R.; Thompson, E. H. Z.; Millar, D. P.; Romesberg, F. E. *J. Phys. Chem. A* **2002**, *106*, 3665–3672.